AGU PUBLICATIONS

Geophysical Research Letters

RESEARCH LETTER
10.1002/2017GL075910

Key Points:
- The Gulf of Alaska was a net carbon sink for 2009
- Low alkalinity tidewater glacial runoff diminishes coastal carbon uptake in summer and fall
- A shift toward higher alkalinity due to increased land-terminating glacial runoff increases carbon uptake by 1.9–2.7 TgC/yr

Supporting Information:
- Supporting Information S1
- Figure S1

Correspondence to:
D. J. Pilcher,
darren.pilcher@noaa.gov

Citation:
Pilcher, D. J., Siedlecki, S. A., Hermann, A. J., Coyle, K. O., Mathis, J. T., & Evans, W. (2018). Simulated impact of glacial runoff on CO_2 uptake in the Gulf of Alaska. *Geophysical Research Letters*, *45*, 880–890. https://doi.org/10.1002/2017GL075910

Received 2 OCT 2017
Accepted 8 JAN 2018
Accepted article online 16 JAN 2018
Published online 30 JAN 2018

Simulated Impact of Glacial Runoff on CO_2 Uptake in the Gulf of Alaska

Darren J. Pilcher[1,2], Samantha A. Siedlecki[1,3], Albert J. Hermann[1,2], Kenneth O. Coyle[4], Jeremy T. Mathis[5], and Wiley Evans[6]

[1]Joint Institute for the Study of the Atmosphere and Ocean, University of Washington, Seattle, WA, USA, [2]Pacific Marine Environmental Laboratory, NOAA, Seattle, WA, USA, [3]Department of Marine Sciences, University of Connecticut, Groton, CT, USA, [4]School of Fisheries and Ocean Sciences, University of Alaska Fairbanks, Fairbanks, AK, USA, [5]NOAA Headquarters, Silver Spring, MD, USA, [6]The Hakai Institute, Heriot Bay, British Columbia, Canada

Abstract The Gulf of Alaska (GOA) receives substantial summer freshwater runoff from glacial meltwater. The alkalinity of this runoff is highly dependent on the glacial source and can modify the coastal carbon cycle. We use a regional ocean biogeochemical model to simulate CO_2 uptake in the GOA under different alkalinity-loading scenarios. The GOA is identified as a current net sink of carbon, though low-alkalinity tidewater glacial runoff suppresses summer coastal carbon uptake. Our model shows that increasing the alkalinity generates an increase in annual CO_2 uptake of 1.9–2.7 TgC/yr. This transition is comparable to a projected change in glacial runoff composition (i.e., from tidewater to land-terminating) due to continued climate warming. Our results demonstrate an important local carbon-climate feedback that can significantly increase coastal carbon uptake via enhanced air-sea exchange, with potential implications to the coastal ecosystems in glaciated areas around the world.

1. Introduction

Although the coastal ocean represents a small percentage of the global ocean area, it contributes disproportionately toward global ocean productivity and carbon uptake relative to its size (Cai, 2011). Quantitative estimates for net carbon uptake remain relatively unconstrained due to difficulties in scaling up limited observational flux data, different definitions of the coastal zone, and spatial heterogeneity between coastal shelves and nearshore regions (Chen & Borges, 2009; Laruelle et al., 2014). Current estimates suggest that continental shelf waters are a weak net sink of 0.19–0.40 PgC/yr (Cai, 2011; Chen et al., 2013; Chen & Borges, 2009; Laruelle et al., 2014). The Gulf of Alaska is considered to be an annual average net sink of 14–34 TgC yr^{-1} (Evans & Mathis, 2013). Significant spatial heterogeneity between the coastal and offshore regions is observed in the GOA, in addition to seasonal periods of both carbon uptake and carbon efflux. Earth system models (ESMs) project a relatively small increase in CO_2 uptake in the GOA over the 21st century (McKinley et al., 2016), but these models are unable to resolve important coastal biogeochemical processes due to their coarse resolution and lack of riverine inputs of carbon and nutrients. Regional models that dynamically downscale ESM output provide finer spatial resolution for robust projections (Hermann et al., 2015; Marshall et al., 2017). One such process that improves with resolution and the addition of regional downscaling is the representation of the freshwater discharge to the ocean (Beamer et al., 2017).

Approximately 47% of the total freshwater discharge into the Gulf of Alaska is derived from glaciers and icefields, with 7–10% attributed to glacier volume loss (Hill et al., 2015; Neal et al., 2010). Both tidewater (i.e., ocean-terminating) and land-terminating glaciers contribute to this glacial runoff, though the relative contribution of each is difficult to constrain, in part because the majority of the runoff comes from distributed small streams as opposed to large river basins (Wang et al., 2004). However, aerial surveys and satellite data can be used to determine the contribution of each glacier type to annual glacier volume loss (as opposed to seasonal melting). Larsen et al. (2015) attributed only 6% of Alaska glacier mass loss from 1994 to 2013 to tidewater glacier melting, and McNabb et al. (2015) reported that ablation rates of Alaskan tidewater glaciers *decreased* from 1985 to 2013. This decrease in tidewater glacier melting despite an increase in atmospheric temperature results from the unique lifecycle of tidewater glaciers. Most Alaska tidewater glaciers have rapidly retreated since the end of the Little Ice Age and are now at a "stable retracted" state, defined by a relative insensitivity to external climate forcing (Larsen et al., 2015; McNabb et al., 2015; Post, 1975). Thus, while

the relative contribution of tidewater and land-terminating glaciers to seasonal glacial runoff is uncertain, it is likely that this composition is shifting toward land-terminating glaciers due to reduced tidewater glacier melting.

This shift in glacial runoff composition from tidewater to land-terminating glaciers has important implications for the coastal carbonate chemistry. Previous GOA studies have connected glacial outflow to corrosive water conditions, defined by relatively lower ratios of total alkalinity (TA)/dissolved inorganic carbon (DIC) (Evans et al., 2014; Reisdorph & Mathis, 2014, 2015). Lower TA/DIC ratios correspond with greater values of pCO_2 and reduced ocean carbon uptake. However, these studies were located in Prince Williams Sound and Glacier Bay, which are predominately impacted by tidewater glacial outflow. Land-terminating glacial runoff can have the opposite effect (i.e., increase TA/DIC ratio) by absorbing geochemically active ions from exposed bedrock, thereby increasing TA (Brown, 2002). This mechanism is particularly strong in streams that flow over sediment recently exposed in the wake of a retreating glacier (Anderson et al., 2000). The GOA drainage basin is composed of a spatially complex mix of carbonate and noncarbonate bedrock (Wilson et al., 2015); however, Anderson (2007) reported high rates of carbonate dissolution in streams draining glaciers on bedrock with only trace carbonate mineral concentrations.

The impact of glacier retreat/advance on rates of chemical weathering in relation to climate change on geologic time frames is an active area of research (Torres et al., 2017), but the transient response of the coastal carbon cycle on much shorter time frames has received relatively little attention. A shift in the composition of glacial runoff to the GOA may increase TA loading to the coastal environment, thereby generating a local carbon-climate feedback that can enhance coastal CO_2 uptake and will likely be applicable to other high-latitude, glaciated regions. For example, studies in Greenland and Svalbard have observed relatively higher TA/DIC ratios and undersaturated pCO_2 values in fjords with significant glacial runoff from land-terminating glaciers (Fransson et al., 2015; Rysgaard et al., 2012). Earth system models do not currently include this process; thus, projections of future carbon uptake within these regions may be underestimated. This will likely also impact projections of ocean acidification, which are critical to constrain because high-latitude coastal regions support some of the largest global fisheries and are particularly vulnerable due to naturally low calcium carbonate concentrations (Fabry et al., 2009; Siedlecki et al., 2017). In this work, we use an existing high-resolution regional model that includes carbon cycling to identify the role of increasing the TA concentration of glacial outflow on spatial and temporal trends in the CO_2 uptake of the GOA, a potentially important carbon-climate currently unresolved by larger scale models.

1.1. Background Oceanography of the GOA

The Gulf of Alaska (GOA) circulation is dominated by the Alaskan Stream and the Alaska Coastal Current (Figure S1 in the supporting information) (Stabeno et al., 2004). A continental shelf divides the GOA into two somewhat distinct systems. The offshore region seaward of the shelf break represents the northern edge of the oligotrophic North Pacific subtropical gyre and is characterized as a high-nutrient, low-chlorophyll system due to iron limitation (Hinckley et al., 2009; Martin et al., 1989). In contrast, the Coastal Gulf of Alaska (CGOA) shoreward of the shelf break is replete with iron due to wind-blown glacial exports (Crusius et al., 2011), glacial freshwater outflow (Wu et al., 2009), and sediment resuspension (Cullen et al., 2009). Cross-shelf transport, curl-driven upwelling, and tidal mixing of nitrate sustain significant productivity within the CGOA, despite downwelling favorable winds (Fiechter & Moore, 2009; Hermann et al., 2009; Stabeno et al., 2004). Productivity in the CGOA is also highly seasonal due to light and temperature limitations typical of a subpolar region. A definitive spring bloom occurs between March-May, with lower but sustained productivity throughout summer when downwelling conditions are relaxed and peak glacial discharge occurs (Coyle et al., 2012). On interannual timescales, both atmospheric and hydrographic features of the GOA are significantly modulated by global patterns such as the El Niño–Southern Oscillation (Hermann et al., 2009, 2016).

2. Methods

2.1. Model Description

We use the Regional Ocean Modeling System (ROMS) (Shchepetkin & McWilliams, 2005; Haidvogel et al., 2008) configured to the GOA (Coyle et al., 2012; Dobbins et al., 2009; Hermann, Hinckley, et al., 2009). This model has a horizontal resolution of 3 km and 42 vertical layers. The physical model is coupled to an

11-component ecosystem model, also previously developed for the GOA (Coyle et al., 2012) This ecosystem model contains two phytoplankton groups (small and large), two microzooplankton groups (small and large), two copepod groups (small and large), and euphausiids. The nutrients traced through the ecosystem model are nitrate, ammonium, and iron. The larger Northeast Pacific Model (NEP) (Curchitser et al., 2005) supplies the boundary conditions and the initial conditions of all model state variables except dissolved inorganic carbon (DIC) and TA. Inclusion of DIC and TA is based on previous implementations within the ROMS framework (Fennel et al., 2008), with modifications for ammonium cycling impacts on the carbon cycle and freshwater influence (Siedlecki et al., 2017).

Lateral boundary and initial conditions for DIC and TA are calculated from empirically derived linear fits to salinity using ship-based observational data from the GOA and Prince Williams Sound (Evans et al., 2014; Siedlecki et al., 2017). There are no observed estimates for the DIC freshwater end-member for the GOA. Therefore, freshwater runoff does not directly impact coastal DIC concentrations in our model formulation, though this simplification neglects additional terrestrial and glacial-derived carbon subsidies. Model sensitivity tests using a constant freshwater DIC value of 1,000 mmolC/m^3 produced similar results, though with a slightly reduced magnitude of change when increasing freshwater TA. This suggests that the model results are robust despite the uncertainty in freshwater DIC. For our initial model implementation we assume no seasonality in the freshwater TA since there is insufficient data to constrain this effect for the GOA, although TA data from different regions (e.g., Columbia and Yukon Rivers) do suggest seasonal variability by a factor of 1.5–2 (Evans et al., 2013; Mathis et al., 2011). A complete description of the model boundary conditions and additional information regarding model sensitivity and uncertainty is provided in the supporting information (Butman & Raymond, 2011; Cooper et al., 2008; Devol & Hedges, 2001; Hood et al., 2009; Hunt et al., 2011; Raymond et al., 2013; Stets et al., 2014; Xue et al., 2016).

2.2. Experimental Setup

We conduct a total of three model simulations that are identical apart from the value of alkalinity present in the freshwater forcing. The "low-alkalinity" scenario has a freshwater TA value of 650 μmol/kg, calculated from the freshwater end-member observed in Prince William Sound (Evans et al., 2014), and is comparable to TA measured near tidewater dominated glacial outflow (Alkire et al., 2015). Thus, we consider this experiment as the "baseline" most representative of tidewater dominated glacial outflow to the GOA system. The "intermediate" and "high-alkalinity" scenarios have freshwater TA values of 1,550 μmol/kg and 1,950 μmol/kg, respectively, and represent the impact of increased TA due to a transition from tidewater to land-terminating glacial freshwater runoff. There are currently no projections for this TA concentration in the GOA, so we select two values that are greater than the current end-member estimate, but constrained to values observed in rivers and glacially fed streams (Table S1). Each model simulation was started from an identical spin-up state, obtained by running the low-alkalinity scenario for a single year using the 2009 forcing. Initial model development determined that 1 year of spin-up was sufficient to ensure stability in the DIC and TA fields. Year 2009 is chosen as the study year due to the availability of high-resolution carbon chemistry data for model validation.

3. Results and Discussion

3.1. Model Performance:

Previous studies have validated physical and biological model variables and identified model biases (Coyle et al., 2012; Hermann, Hinckley, et al., 2009; Hinckley et al., 2009). Briefly, stratification on the coastal shelf is likely too strong, resulting in reduced vertical nutrient flux, an earlier seasonal depletion of nitrate, and reduced biological productivity. Model salinity is also biased high by 1–2 practical salinity units, possibly due to initial and boundary conditions from the NEP model. This bias was accounted for when generating the initial and boundary conditions for TA and DIC (Siedlecki et al., 2017). Model DIC, TA, and pCO_2 are compared to observational data collected along the Northeast Pacific Global Ocean Ecosystems Dynamics Seward line transect (Figure S3). Model DIC, TA, and pCO_2 compare favorably to the observations, though TA is consistently biased high, particularly at the surface. Although the overestimate of TA does not currently lead to a significant low bias in pCO_2, any further bias may rapidly generate a bias in pCO_2 due to nonlinearity in the carbonate system. The model also tends to simulate reduced variability compared to

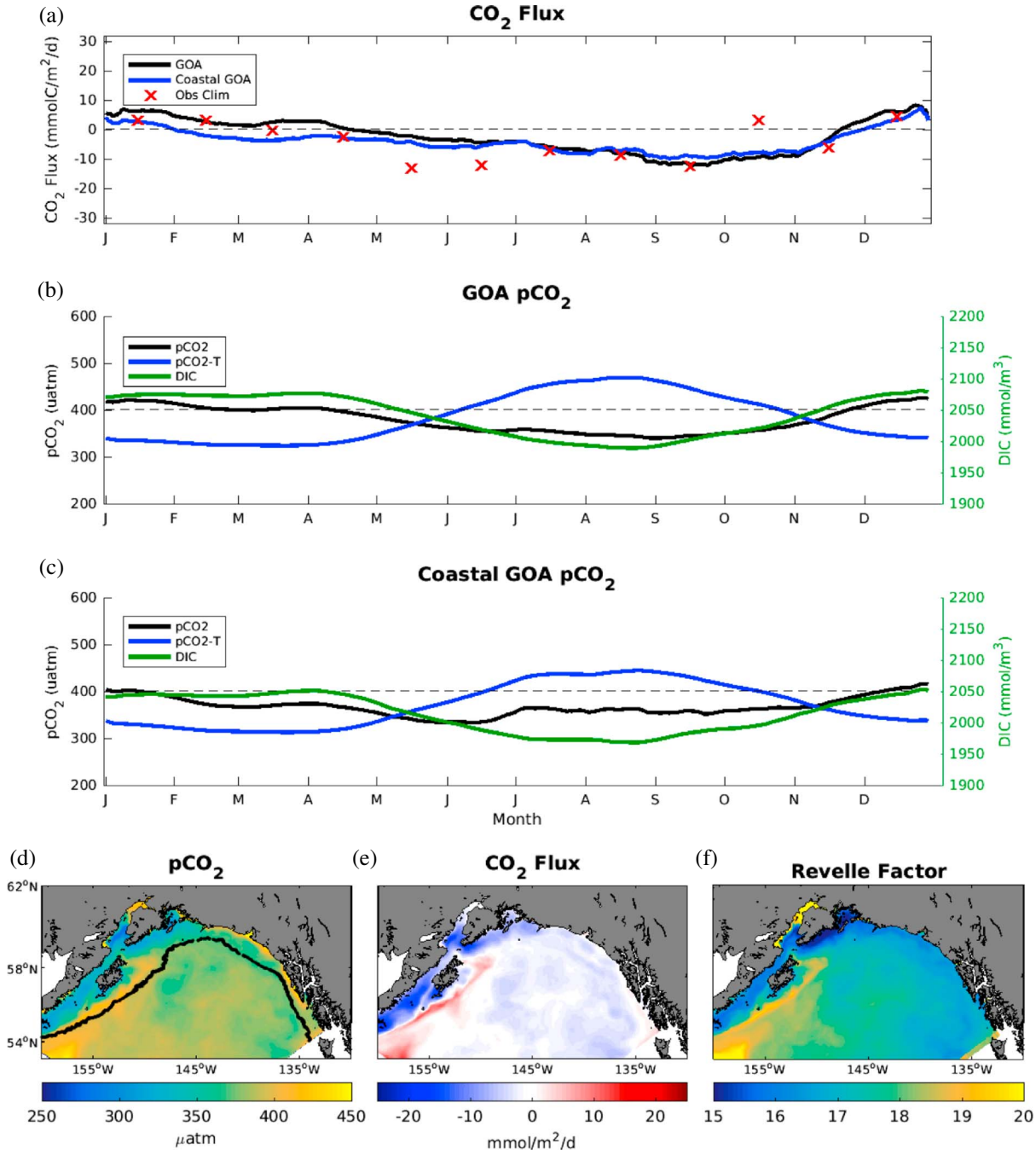

Figure 1. (a) Time series of area-weighted spatial mean model CO_2 flux for the entire model domain (black solid line) and the coastal domain (blue solid line). The red tick marks denote climatological values reported by Evans and Mathis (2013). A negative CO_2 flux value represents a flux of carbon into the ocean. Time series of area-weighted spatial mean model pCO_2 (black solid line), pCO_2-T calculated from equation (1) (blue line), and surface DIC (green line) for both (b) the entire model domain and (c) the coastal domain. Also shown is the model value of atmospheric pCO_2 (blacked dashed line). Annual average surface (d) pCO_2, (e) CO_2 flux, and (f) Revelle factor. The black outline in Figure 1d represents the 1,500 m isobath that constrains the Coastal Gulf of Alaska. The model output for Figures 1a–1c was smoothed using a 30 day filter.

the observations. A complete description of model validation is provided in Text S2 (Jolliff et al., 2009; Stow et al., 2009).

We find that the Gulf of Alaska was an annual average carbon sink of 2.3 mmolC/m^2/d for 2009 (Figure 1a). The Coastal Gulf of Alaska was an annual average carbon sink of 4.0 mmolC/m^2/d, which is identical to the

climatological observed value reported by Evans and Mathis (2013). Scaling these values to surface area produces a net carbon uptake of 10.6 TgC/yr for the entire GOA and 5.3 TgC/yr for the Coastal GOA. These values are lower than the 14–36 TgC/yr range reported by Evans and Mathis (2013) due to the smaller total surface area of our model domain. Seasonally, the GOA alternates between net carbon efflux from mid-November through mid-February and net carbon uptake for the remainder of the year. This seasonal cycle is very similar to the observed climatology despite the substantial difference in spatial and temporal resolution. For example, climatological CO_2 flux in May-June is more than twice as great in magnitude compared to the model (-12 and -13 mmolC/m^2/d observed compared to -2.5 and -4.0 mmolC/m^2/d modeled); however, these observed data are predominately located near the Kenai Peninsula and southwestern Alaskan coastline (Evans & Mathis, 2013). This is a region of high-magnitude CO_2 uptake in the model as well, but this signal is diluted when averaged across the entire model spatial domain. Similarly, October is a clear outlier in the observed climatology due to heavy sampling of waters supersaturated with carbon in the Alexander Archipelago region along the southeastern Alaskan coastline. Elsewhere, CO_2 flux values remain negative, suggesting that the climatological value is biased high by the Alexander Archipelago, a region that is not resolved in the model.

The summer-fall time frame is also when model CO_2 flux is nearly identical between the GOA and CGOA. These model values also closely agree with the observed climatology. This suggests that the model coastal flux values and the observed climatology are a robust estimate of CO_2 uptake for not only the coastal GOA but also for the entire GOA during this time frame. Future observational campaigns can exploit this result by focusing summer sampling locations within coastal regions.

3.2. Seasonal Drivers of pCO_2

Ocean carbon uptake occurs when the partial pressure of CO_2 in surface seawater (pCO_2) is less than the atmosphere. To examine seasonal variability in carbon uptake, we compare the seasonal pCO_2 cycle with surface DIC concentrations, and the temperature component of pCO_2 (pCO_2-T) in coastal and offshore regions (Figures 1b and 1c). The temperature component represents the effect of thermal solubility on pCO_2 (i.e., colder seawater has a greater capacity for gas uptake) and is calculated by an empirically derived formula from Takahashi et al. (2002):

$$pCO_2 - T = \overline{pCO_2} \times \exp\left[0.0423\left(T - \overline{T}\right)\right] \quad (1)$$

where overbars denote the annual mean. Thus, an increase in temperature generates an increase in pCO_2 and vice versa.

For the GOA, area-weighted spatial mean pCO_2 is strongly correlated with surface DIC ($r = 0.93$, p-value < 0.01) but is also seasonally modulated by thermal solubility (Figures 1b and 1c). These two processes are directly out of phase and have a competing impact on pCO_2. During winter and spring months, elevated DIC concentrations act to increase pCO_2 while lower water temperatures decrease pCO_2. Conversely, warmer temperatures decreased pCO_2 during the summer and fall months. Despite the competing impact of temperature, the pCO_2 cycle closely mirrors that of DIC, suggesting that surface DIC is the primary driver of the seasonal carbon cycle. Figure 1c illustrates a similar seasonal cycle in the CGOA for pCO_2-T and DIC; however, the correlation between pCO_2 and DIC ($r = 0.49$, p-value < 0.01) is not as strong as for the GOA. This decreased correlation results from the June-October months, when pCO_2 increases despite seasonal minimum in surface DIC. pCO_2-T is at a seasonal maximum during these months, so this may be partly responsible for the decoupling between DIC and pCO_2. However, this decoupling is not present for the GOA, despite a greater pCO_2-T component (Figure 1b). This suggests that there may be additional mechanisms that have a greater impact on summer-fall pCO_2 in the CGOA.

3.3. Spatial Variability of pCO_2

Ocean carbon uptake primarily occurred on the continental shelf (<1,500 m) and the northeastern offshore basin between 135°W and 148°W (Figures 1d and 1e). The most intense annual negative CO_2 flux values (i.e., net carbon uptake by the ocean) are concentrated along the southwestern Alaskan coastline and are driven by low pCO_2 values (50–150 μatm lower than the atmosphere). Positive CO_2 flux values (i.e., net carbon efflux to the atmosphere) are limited to the southwestern GOA basin and regions surrounding Kodiak Island and correspond to supersaturated pCO_2 values and strong wind speeds (Figure S4). The Revelle factor

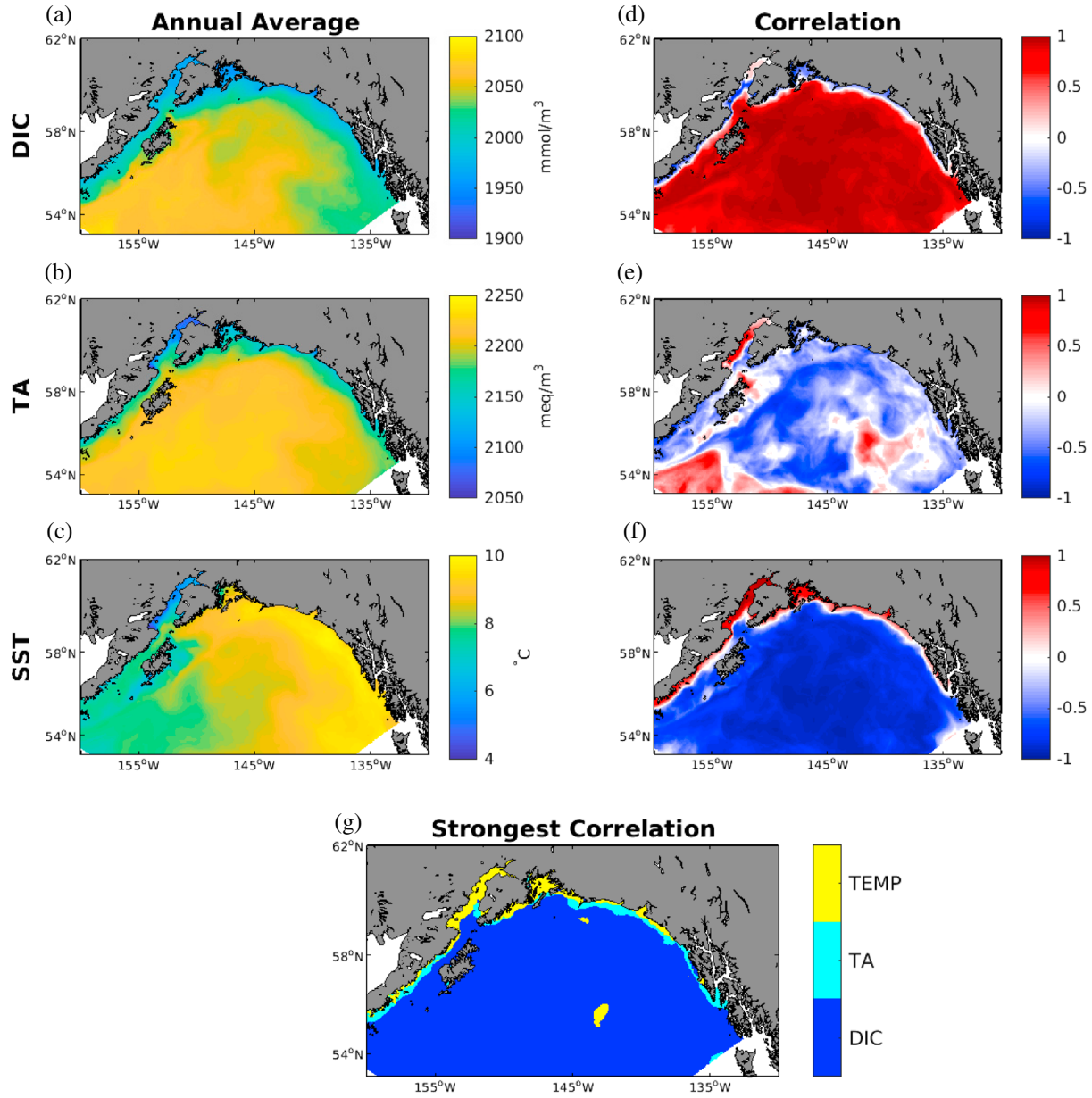

Figure 2. Annual average values of (a) DIC, (b) TA, and (c) SST and spatial correlations at each model point between pCO_2 and (d) DIC, (e) TA, and (f) SST. Also shown is (g) the largest magnitude (positive or negative) correlation at each point. Only correlations with a *p*-value less than 0.05 are shown.

measures the capacity of the ocean to absorb atmospheric CO_2, with lower numbers equating to increased uptake capacity. We calculate the Revelle factor from DIC and TA using the following approximation from Sarmiento and Gruber (2006):

$$RF \approx \frac{3 \cdot Alk \cdot DIC - 2 \cdot DIC^2}{(2 \cdot DIC - Alk)(Alk - DIC)} \quad (2)$$

The Revelle factor is lowest in the regions of greatest ocean carbon uptake and highest in regions of net carbon efflux (Figure 1f). Comparing Figures 1d–1f illustrates that negative CO_2 flux values occur in regions with undersaturated pCO_2 values and a lower Revelle factor. This showcases that the spatial variability in GOA carbon uptake is driven by the ocean capacity for carbon uptake. The spatial variability in the Revelle factor is driven by variability in both DIC and TA.

Annual average DIC is lower in the CGOA compared to the GOA, consistent with a lower Revelle factor (Figure 2a). TA is also relatively low in these coastal regions, though the impact of DIC on reducing the Revelle factor is generally greater. In the offshore basin, there is a longitudinal gradient of increasing DIC and TA when moving east-to-west that is similar to the longitudinal gradient in the Revelle factor and CO_2 flux. Sea surface temperature (SST) also displays a longitudinal gradient of decreasing values to the west, which further supports increased carbon uptake via increased gas solubility (Figure 2c).

Figure 1 suggests that surface DIC is the primary driver of pCO_2 for the GOA, but that the correlation is not as strong within the CGOA. Figure 2 shows spatial correlations of pCO_2 with surface DIC, TA, and temperature, as well as the greatest magnitude spatial correlation. Consistent with Figure 1, surface DIC has a strongly positive correlation with pCO_2 throughout most of the GOA, except for nearshore regions within the 1,500 m isobath. Here the correlations with DIC range from −0.7 to 0.9. These areas are also negatively correlated with TA and positively correlated with temperature (Figures 2e and 2f). Thus, the coastal region is defined by an interplay between DIC, TA, and temperature (Figure 2g). The latter two processes have a much greater impact during the summer, when coastal pCO_2 increases due to an increase in temperature and decrease in TA (Figure S5). The decrease in TA occurs in regions of high freshwater runoff and decreased summer salinity. The low alkalinity freshwater end-member therefore reduces coastal summer TA, resulting in a reduced capacity for ocean carbon uptake. A similar process occurs in Glacier Bay, Alaska, and Prince Williams Sound, where freshwater runoff low in TA reduces buffering capacity (Evans et al., 2014; Reisdorph & Mathis, 2014). This process is sensitive to the TA of the freshwater end-member, which is derived from a linear relationship between alkalinity and salinity measurements taken within Prince Williams Sound (Evans et al., 2014). This freshwater end-member is highly uncertain and may be biased high, based on limited low salinity data that were excluded from the regression and the relatively greater values of modeled TA compared to observations. A lower TA freshwater end-member would further suppress summer coastal carbon uptake, though the current model estimates are consistent with the observed climatology.

3.4. Impact of Alkalinity in the Freshwater End-Member

We ran two additional model experiments with increased alkalinity in the freshwater runoff to simulate the effect of a transition in glacial contribution to the freshwater flux and determine the net impact of those changes on CO_2 flux. The modified freshwater forcing increases coastal TA and decreases pCO_2, thereby generating enhanced ocean carbon uptake (Figure 3). These changes are spatially constrained to the CGOA. These regions experience a pCO_2 decrease from winter to summer, and the modified freshwater forcing reduces and often eliminates this decrease (Figure S5). This results in a significant enhancement of carbon uptake following increased summer freshwater runoff.

The three simulations have similar average coastal CO_2 flux values through the first half of the year, but begin to diverge by early June (Figure 3g). This effect continues to grow through the fall, resulting in a 85% and 118% increase in November coastal CO_2 flux for the "intermediate-alkalinity" and high-alkalinity respective simulations and a sign reversal from net efflux to net uptake in December. Annual mean coastal CO_2 flux is enhanced from −4.0 mmolC/m^2/d in the low-alkalinity simulation to −5.4 mmolC/m^2/d and −6.0 mmolC/m^2/d in the midalkalinity and high-alkalinity simulations, respectively. This constitutes a 34–48% increase in total carbon uptake of 1.8–2.5 TgC/yr for the CGOA and a 18–25% increase in total carbon uptake of 1.9–2.7 TgC/yr for the entire GOA. The increase in carbon uptake is not spatially uniform, but rather concentrated shoreward of the 1,500 m isobath and also east of Prince Williams Sound where modeled and observed freshwater discharge is greater (Figure S6). June–November mean coastal carbon uptake increases by 3.3–4.5 mmolC/m^2/d for the coastal region east of 148°W, but increases by only 1.1–1.5 mmolC/m^2/d for the region west of 148°W. Thus, the freshwater alkalinity runoff is acting to reduce and reverse the longitudinal gradient in CO_2 flux that is present in the 2009 hindcast simulation (Figures 1d and 1e). The region of most intense carbon uptake shifts from the coastal zone west of 148°W to the coastal zone east of 148°W. The increase in carbon uptake is approximately linear (~0.1 mmolC/m^2/d increase in carbon uptake per 65 μmol/kg increase in TA for both experiments), suggesting that this mechanism is not nearing saturation in the high-alkalinity scenario, though this may change on longer time frames.

This mechanism is just one of a growing number of important links between the glacial-ocean interface and the coastal ecosystem (O'Neel et al., 2015). Many of these systems are undergoing rapid changes due to

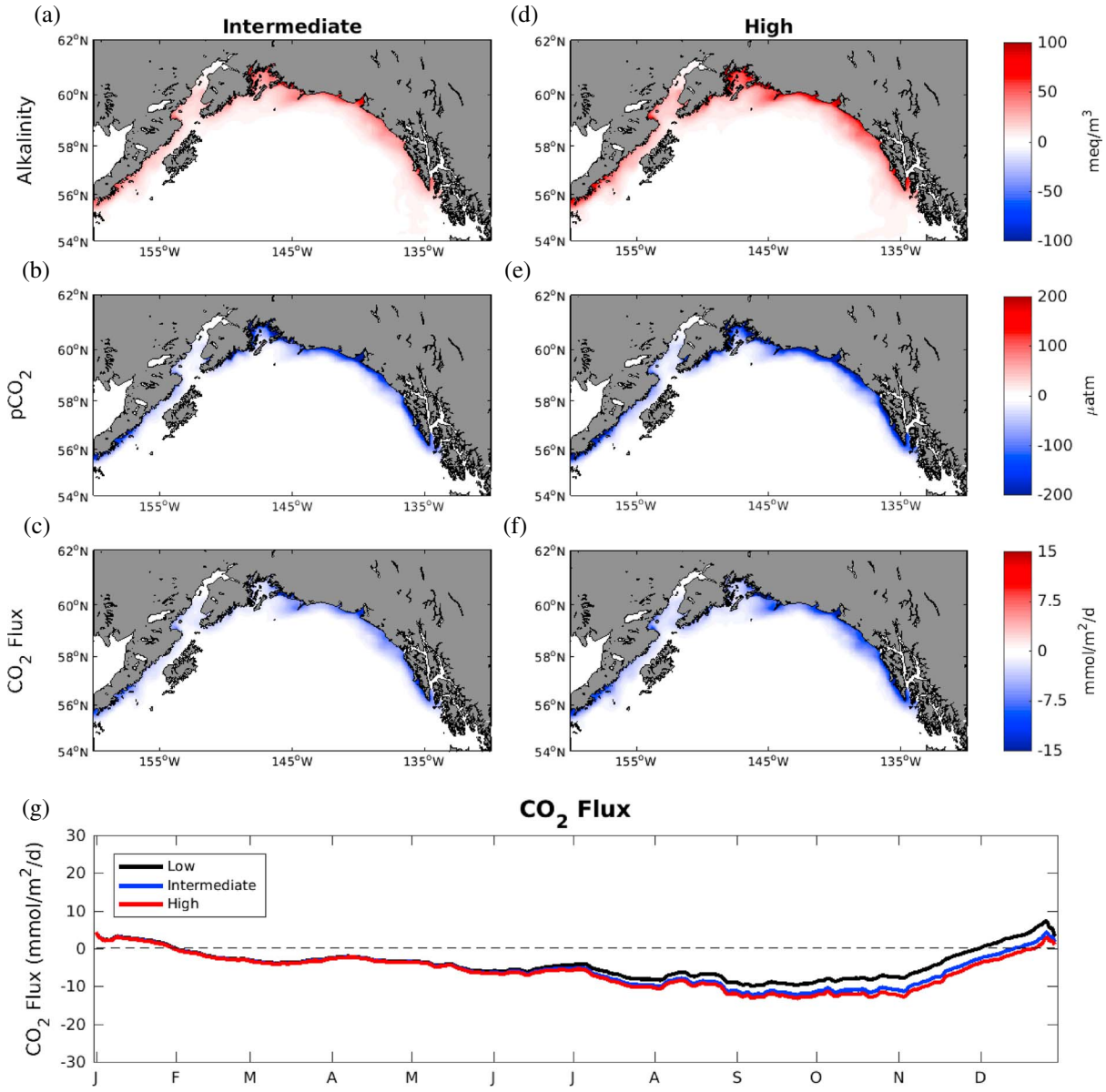

Figure 3. (a–f) Difference plots between the "intermediate" (1,550 μmol/kg) and high-alkalinity (1,950 μmol/kg) scenarios and the low alkalinity (650 μmol/kg) scenario, where a positive value indicates an increase in compared to the low-alkalinity scenario. All variables are averaged over the June-October time frame. (g) Time series of coastal area-weighted spatial mean CO_2 flux for the low-alkalinity scenario (solid black line) and the intermediate (blue line) and high-alkalinity (red line) scenarios.

climate change. Glacial runoff is projected to decrease with climate change; however, total freshwater runoff to the GOA is projected to increase due to an increase in precipitation (Beamer et al., 2017; Larsen et al., 2015). Increased precipitation along with melting permafrost can mobilize additional terrestrial carbon into Alaskan streams (O'Donnell et al., 2016; Smits et al., 2017). These processes may generate an increase in terrestrial carbon export to the coastal ocean, which would counter the glacial runoff export of TA.

4. Conclusions

The Gulf of Alaska was a net carbon sink carbon for 2009, consistent with observed climatological estimates. Carbon uptake was strongest in coastal regions lying west of 148°W due to enhanced carbon uptake capacity driven by relatively low concentrations of DIC. The seasonal carbon cycle is strongly correlated with the seasonal cycle of DIC, except in coastal regions. These areas are also impacted by temperature and

alkalinity, particularly during the summer when freshwater runoff low in TA reduces coastal carbon uptake. The model results suggest that a shift from a tidewater to a land-terminating glacier dominated system will increase coastal ocean CO_2 uptake. This mechanism constitutes a carbon-climate feedback, similar to the geologic process of chemical weathering, and is currently not included in global Earth system models. We provide the first extrapolation of this impact to an entire coastal ocean system. Including this mechanism increases annual mean carbon uptake by 1.9–2.7 TgC/yr (18–25% increase), with the greatest increase occurring adjacent to heavily glaciered regions of the Alaskan coast. This is consistent with previous studies showing increased carbon uptake near glacial outflow in Greenland and Svalbard. We speculate that our results may be representative of high-latitude glacial regions outside of the Gulf of Alaska and recommend further sampling of carbon chemistry variables in glacial outflow. The effects suggested here have a significant impact on the regional carbon budget as well as implications for regional fisheries sensitive to ocean acidification (Siedlecki et al., 2017). This mechanism may therefore be important for projecting coastal ecosystem impacts associated with the continued oceanic uptake of atmospheric CO_2.

Acknowledgments
Model simulations and analysis were performed using the University of Washington Hyak supercomputer system, supported in part by the University of Washington eScience Institute. Observational data are available through AOOS (http://portal.aoos.org/alaska-statewide#), NOAA PMEL (www.pmel.noaa.gov/co2/), and CDIAC (http://cdiac.ornl.gov). Model fields are available in the University of Washington Libraries' ResearchWorks repository (https://doi.org/10.6069/H5C82790). This research was performed while D.J. P. held a National Research Council Research Associateship award at the Pacific Marine Environmental Laboratory. Funding was also provided by the Regional U.S. Integrated Ocean Observing System (IOOS), the Alaska Ocean Observing System (AOOS), and through the Joint Institute for the Study of the Atmosphere and Ocean (JISAO) NOAA cooperative agreement NA10OAR4320148 (2010–2015) and NA15OAR4320063 (2015–2020). We thank two anonymous reviewers for their helpful comments, which greatly improved this manuscript. This is PMEL contribution number 4596.

References

Alkire, M. B., Nilsen, F., Falck, E., Søreide, J., & Gabrielsen, T. M. (2015). Tracing sources of freshwater contributions to first-year sea ice in Svalbard fjordss. *Continental Shelf Research*, *101*, 85–97. https://doi.org/10.1016/j.csr.2015.04.003

Anderson, S. P. (2007). Biogeochemistry of glacial landscape systems. *Annual Review of Earth and Planetary Sciences*, *35*, 375–379. https://doi.org/10.1146/annurev.earth.35.031306.140033

Anderson, S. P., Drever, J. I., Frost, C. D., & Holden, P. (2000). Chemical weathering in the foreland of a retreating glacier. *Geochimica et Cosmochimica Acta*, *64*(7), 1173–1189.

Beamer, J. P., Hill, D. F., McGrath, D., Arendt, A., & Kienholz, C. (2017). Hydrologic impacts of changes in climate and glacier extent in the Gulf of Alaska watershed. *Water Resources Research*, *53*, 7502–7520. https://doi.org/10.1002/2016WR020033

Brown, G. H. (2002). Glacier meltwater hydrochemistry. *Applied Geochemistry*, *17*, 855–883.

Butman, D., & Raymond, P. A. (2011). Significant efflux of carbon dioxide from streams and rivers in the United States. *Nature Geoscience*, *4*, 839–842. https://doi.org/10.1038/NGEO1294

Cai, W.-J. (2011). Estuarine and coastal ocean carbon paradox: CO_2 sinks or sites of terrestrial carbon incineration? *Annual Review of Marine Science*, *3*, 123–145. https://doi.org/10.1146/annurev-marine-120709-142723

Chen, C.-T. A., & Borges, A. V. (2009). Reconciling opposing views on carbon cycling in the coastal ocean: Continental shelves as sinks and near-shore ecosystems as sources of atmospheric CO_2. *Deep-Sea Research Part II*, *56*, 578–590. https://doi.org/10.1016/j.dsr2.2009.01.001

Chen, C.-T. A., Huang, T.-H., Chen, Y.-C., Bai, Y., He, X., & Kang, Y. (2013). Air-sea exchanges of CO_2 in the world's coastal seas. *Biogeosciences*, *10*, 6509–6544. https://doi.org/10.5194/bg-10-6509-2013

Cooper, L. W., McClelland, J. W., Holmes, R. M., Raymond, P. A., Gibson, J. J., Guay, C. K., & Peterson, B. J. (2008). Flow-weighted values of runoff tracers ($\delta^{18}O$, DOC, Ba, alkalinity) from the six largest Arctic rivers. *Geophysical Research Letters*, *35*, L18606. https://doi.org/10.1029/2008GL035007

Coyle, K. O., Cheng, W., Hinckley, S. L., Lessard, E. J., Whitledge, T., Hermann, A. J., & Hedstrom, K. (2012). Model and field observations of effects of circulation on the timing and magnitude of nitrate utilization and production on the northern Gulf of Alaska shelf. *Progress in Oceanography*, *103*, 16–41. https://doi.org/10.1016/j.pocean.2012.03.002

Crusius, J., Schroth, A. W., Gassó, S., Moy, C. M., Levy, R. C., & Gatica, M. (2011). Glacial flour dust storms in the Gulf of Alaska: Hydrologic and meteorological controls and their importance as a source of bioavailable iron. *Geophysical Research Letters*, *38*, L06602. https://doi.org/10.1029/2010GL046573

Cullen, J. T., Chong, M., & Ianson, D. (2009). British Columbian continental shelf as a source of dissolved iron to the subarctic northeast Pacific Ocean. *Global Biogeochemical Cycles*, *23*, GB4012. https://doi.org/10.1029/2008GB003326

Curchitser, E. N., Haidvogel, D. B., Hermann, A. J., Dobbins, E. L., Powell, T. M., & Kaplan, A. (2005). Multi-scale modeling of the North Pacific Ocean: Assessment and analysis of simulated basin-scale variability (1996–2003). *Geophysical Research Letters*, *110*, C11021. https://doi.org/10.1029/2005JC002902

Devol, A. H., & Hedges, J. I. (2001). Organic matter and nutrients in the mainstem Amazon River. In M. E. McClain, R. L. Victoria, & J. E. Richey (Eds.), *The biogeochemistry of the Amazon Basin* (pp. 275–306). New York: Oxford University Press.

Dobbins, E. L., Hermann, A. J., Stabeno, P., Bond, N. A., & Steed, R. C. (2009). Modeled transport of freshwater from a line-source in the coastal Gulf of Alaska. *Deep-Sea Research Part II*, *56*, 2409–2426. https://doi.org/10.1016/j.dsr2.2009.02.004

Evans, W., Hales, B., & Strutton, P. G. (2013). pCO_2 distributions and air-water CO_2 fluxes in the Columbia River estuary. *Estuarine, Coastal and Shelf Science*, *117*, 260–272. https://doi.org/10.1016/j.ecss.2012.12.003

Evans, W., & Mathis, J. T. (2013). The Gulf of Alaska coastal ocean as an atmospheric CO_2 sink. *Continental Shelf Research*, *65*, 52–63. https://doi.org/10.1016/j.csr.2013.06.013

Evans, W., Mathis, J. T., & Cross, J. N. (2014). Calcium carbonate corrosivity in an Alaskan inland sea. *Biogeosciences*, *11*, 365–379. https://doi.org/10.5194/bg-11-365-2014

Fabry, V. J., McClintock, J. B., Mathis, J. T., & Grebmeier, J. M. (2009). Ocean acidification at high latitudes: The bellwether. *Oceanography*, *22*(4), 160–171.

Fennel, K., Wilkin, J., Previdi, M., & Najjar, R. (2008). Denitrification effects on air-sea CO_2 flux in the coastal ocean: Simulations for the northwest North Atlantic. *Geophysical Research Letters*, *35*, L24608. https://doi.org/10.1029/2008GL036147

Fiechter, J., & Moore, A. M. (2009). Interannual spring bloom variability and Ekman pumping in the Coastal Gulf of Alaska. *Journal of Geophysical Research*, *114*, C06004. https://doi.org/10.1029/2008JC00514

Fransson, A., Chierici, M., Nomura, D., Granskog, M. A., Kristiansen, S., Martma, T., & Nehrke, G. (2015). Effect of glacial drainage water on the CO_2 system and ocean acidification state in an Arctic tidewater-glacier fjord during two contrasting years. *Journal of Geophysical Research: Oceans*, *120*, 2413–2429. https://doi.org/10.1002/2014JC010320

Haidvogel, D. B., Arango, H., Budgell, W. P., Cornuelle, B. D., Curchitser, E., di Lorenzo, E., … Wilkin, J. (2008). Ocean forecasting in terrain-following coordinates: formulation and skill assessment of the Regional Ocean Modeling System. *Journal of Computational Physics*, *227*(7), 3595–3624. https://doi.org/10.1016/j.jcp.2007.06.016

Hermann, A. J., Curchitser, E. N., Haidvogel, D. B., & Dobbins, E. L. (2009). A comparison of remote vs. local influence of El Niño on the coastal circulation of the northeast Pacific. *Deep-Sea Research Part II*, *56*, 2427–2443. https://doi.org/10.1016/j.dsr2.2009.02.005

Hermann, A. J., Gibson, G. A., Bond, N. A., Curchitser, E. N., Hedstrom, K., Cheng, W., … Aydin, K. (2015). Projected future biophysical states of the Bering Sea. *Deep-Sea Research Part II*, *134*, 30–47. https://doi.org/10.1016/j.dsr2.2015.11.001

Hermann, A. J., Hinckley, S., Dobbins, E. L., Haidvogel, D. B., Bond, N. A., Mordy, C., … Stabeno, P. J. (2009). Quantifying cross-shelf and vertical nutrient flux in the Coastal Gulf of Alaska with a spatially nested, coupled biophysical model. *Deep-Sea Research Part II*, *56*, 2474–2486. https://doi.org/10.1016/j.dsr2.2009.02.008

Hermann, A. J., Ladd, C., Cheng, W., Curchitser, E. N., & Hedstrom, K. (2016). A model-based examination of multivariate physical modes in the eastern and western Gulf of Alaska. *Deep-Sea Research Part II*, *132*, 68–89. https://doi.org/10.1016/j.dsr2.2016.04.005i

Hill, D. F., Bruhis, N., Calos, S. E., Arendt, A., & Beamer, J. (2015). Spatial and temporal variability of freshwater discharge into the Gulf of Alaska. *Journal of Geophysical Research: Oceans*, *120*, 634–646. https://doi.org/10.1002/2014JC010395

Hinckley, S., Coyle, K. O., Gibson, G., Hermann, A. J., & Dobbins, E. L. (2009). A biophysical NPZ model with iron for the Gulf of Alaska: Reproducing the differences between an oceanic HNLC ecosystem and a classical northern temperature shelf ecosystem. *Deep-Sea Research Part II*, *56*, 2520–2536. https://doi.org/10.1016/j.dsr2.2009.03.003

Hood, E., Fellman, J., Spencer, R. G. M., Hernes, P. J., Edwards, R., D'Amore, D., & Scott, D. (2009). Glaciers as a source of ancient and labile organic matter to the marine environment. *Nature*, *463*, 1044–1048. https://doi.org/10.1038/nature08580

Hunt, C. W., Salisbury, J. E., & Vandemark, D. (2011). Contribution of non-carbonate anions to total alkalinity and overestimation of pCO_2 in New England and New Brunswick rivers. *Biogeosciences*, *8*, 3069–3076. https://doi.org/10.5194/bg-8-3069-2011

Jolliff, J. K., Kindle, J. C., Shulman, I., Penta, B., Friedrichs, M. A. M., Helber, R., & Arnone, R. A. (2009). Summary diagrams for coupled hydrodynamic-ecosystem model skill assessment. *Journal of Marine Systems*, *76*, 64–82. https://doi.org/10.1016/j.jmarsys.2008.05.014

Larsen, C. F., Burgess, E., Arendt, A. A., O'Neel, S., Johnson, A. J., & Kienholz, C. (2015). Surface melt dominates Alaska glacier mass balance. *Geophysical Research Letters*, *42*, 5902–5908. https://doi.org/10.1002/2015GL064349

Laruelle, G. G., Lauerwald, R., Pfeil, B., & Regnier, P. (2014). Regionalized global budget of the CO_2 exchange at the air-water interface in continental shelf seas. *Global Biogeochemical Cycles*, *28*, 1199–1214. https://doi.org/10.1002/2014GB004832

Marshall, K. N., Kaplan, I. C., Hodgson, E. E., Hermann, A. J., Busch, S., McElhany, P., … Fulton, E. A. (2017). Risks of ocean acidification in the California Current food web and fisheries: Ecosystem model projections. *Global Change Biology*, *23*, 1525–1539. https://doi.org/10.1111/gcb.13594

Martin, J. H., Gordon, R. M., Fitzwater, S., & Broenkow, W. W. (1989). VERTEX: phytoplankton/iron studies in the Gulf of Alaska. *Deep Sea Research*, *36*, 649–680.

Mathis, J. T., Cross, J. N., & Bates, N. R. (2011). Coupling primary production and terrestrial runoff to ocean acidification and carbonate mineral suppression in the eastern Bering Sea. *Journal of Geophysical Research*, *116*, C02030. https://doi.org/10.1029/2010JC006453

McKinley, G. A., Pilcher, D. J., Fay, A. R., Lindsay, K., Long, M. C., & Lovenduski, N. S. (2016). Timescales for detection of trends in the ocean carbon sink. *Nature*, *530*, 469–472. https://doi.org/10.1038/nature16958

McNabb, R. W., Hock, R., & Huss, M. (2015). Variations in Alaska tidewater glacier frontal ablation, 1985-2013. *Journal of Geophysical Research; Earth Surface*, *120*, 120–136. https://doi.org/10.1002/2014JF003276

Neal, E. G., Hood, E., & Smikrud, K. (2010). Contribution of glacier runoff to freshwater discharge into the Gulf of Alaska. *Geophysical Research Letters*, *37*, L06404. https://doi.org/10.1029/2010GL042385

O'Donnell, J. A., Aiken, G. R., Swanson, D. K., Panda, S., Butler, K. D., & Baltensperger, A. P. (2016). Dissolved organic matter composition of Arctic rivers: Linking permafrost and parent material to riverine carbon. *Global Biogeochemical Cycles*, *30*, 1811–1826. https://doi.org/10.1002/2016GB005482

O'Neel, S., Hood, E., Bidlack, A. L., Fleming, S. W., Arimitsu, M. L., Arendt, A., … Pyare, S. (2015). Icefield-to-ocean linkages across the northern Pacific coastal temperate rainforest ecosystem. *Bioscience*, *65*(5), 499–512.

Post, A. (1975). Preliminary hydrography and historic terminal changes of Columbia Glacier, Alaska, U.S. Geol. Surv. Hydrol. Invest. Atlases, 559, 3 sheets, scale 1:20,000.

Raymond, P. A., Hartmann, J., Lauerwald, R., Sobek, S., McDonald, C., Hoover, M., … Guth, P. (2013). Global carbon dioxide emissions from inland waters. *Nature*, *503*, 355–359. https://doi.org/10.1038/nature12760

Reisdorph, S. C., & Mathis, J. T. (2014). The dynamic controls on carbonate mineral saturation states and ocean acidification in a glacially dominated estuary. *Estuarine, Coastal and Shelf Science*, *144*, 8–18. https://doi.org/10.1016/j.ecss.2014.03.018

Reisdorph, S. C., & Mathis, J. T. (2015). Assessing net community production in a glaciated Alaskan fjord. *Biogeosciences*, *12*, 5185–5198. https://doi.org/10.5194/bg-12-5185-2015

Rysgaard, S., Mortensen, J., Juul-Pedersen, T., Sørensen, L. L., Lennert, K., Søgaard, D. H., … Bendtsen, J. (2012). High air-sea CO_2 uptake rates in nearshore and shelf areas of Southern Greenland: Temporal and spatial variability. *Marine Chemistry*, *128-129*, 26–33. https://doi.org/10.1016/j.marchem.2011.11.002

Sarmiento, J. L., & Gruber, N. (2006). *Ocean biogeochemical dynamics*, (p. 526). Princeton, NJ: Princeton University Press.

Shchepetkin, A. F., & McWilliams, J. C. (2005). The regional oceanic modeling system (ROMS): A split-explicit, free-surface, topography-following-coordinate oceanic model. *Ocean Modelling*, *9*, 347–404. https://doi.org/10.1016/j.ocemod.2004.08.002

Siedlecki, S. A., Pilcher, D. J., Hermann, A., Coyle, K., & Mathis, J. T. (2017). The importance of freshwater to spatial variability of aragonite saturation state in the Gulf of Alaska. *Journal of Geophysical Research: Oceans*, *122*, 8482–8502. https://doi.org/10.1002/2017JC012791

Smits, A. P., Schindler, D. E., Holtgrieve, G. W., Jankowski, K. J., & French, D. W. (2017). Watershed geomorphology interacts with precipitation to influence the magnitude and source of CO_2 emissions from Alaskan streams. *Journal of Geophysical Research: Biogeosciences*, *122*, 1903–1921. https://doi.org/10.1002/2017JG003792

Stabeno, P. J., Bond, N. A., Hermann, A. J., Mordy, C. W., & Overland, J. E. (2004). Meteorology and Oceanography of the Northern Gulf of Alaska. *Continental Shelf Research*, *24*, 859–897.

Stets, E. G., Kelly, V. J., & Crawford, C. G. (2014). Long-term trends in alkalinity in large rivers of the conterminous US in relation to acidification, agriculture, and hydrologic modification. *Science of the Total Environment*, *488-489*, 280–289. https://doi.org/10.1016/j.scitotenv.2014.04.054

Stow, C. A., Jolliff, J., McGillicuddy, D. J., Doney, S. C., Allen, J. I., Friedrichs, M. A. M., … Wallhead, P. (2009). Skill assessment for coupled biological/physical models of marine systems. *Journal of Marine Systems*, *76*(1–2), 4–15. https://doi.org/10.1016/j.jmarsys.2008.03.011

Takahashi, T., Sutherland, S. C., Sweeney, C., Poisson, A., Metzl, N., Tilbrook, B., … Nojiri, Y. (2002). Global sea-air CO_2 flux based on climatological surface ocean pCO_2 and seasonal biological and temperature effects. *Deep-Sea Research Part II*, *49*, 1601–1622.

Torres, M. A., Moosdorf, N., Hartmann, J., Adkins, J. F., & West, A. J. (2017). Glacial weathering, sulfide oxidation, and global carbon cycle feedbacks. *Proceedings of the National Academy of Sciences of the United States of America*, *114*, 8716–8721. https://doi.org/10.1073/pnas.1702953114

Wang, J. M., Jin, M., Musgrave, D. L., & Ikeda, M. (2004). A hydrological digital elevation model for freshwater discharge into the Gulf of Alaska. *Journal of Geophysical Research*, *109*, C07009. https://doi.org/10.1029/2002JC001430

Wilson, F. H., Hults, C. P., Mull, C. G., & Karl, S. M. (2015). *Geologic map of Alaska: U.S. Geologic Survey Scientific Invesitgations Map 3340* (p. 197). Reston, VA. https://doi.org/10.3133/sim3340

Wu, J., Aguilar-Islas, A., Rember, R., Weingartner, T., Danielson, S., & Whitledge, T. (2009). Size-fractionated iron distribution on the northern Gulf of Alaska. *Geophysical Research Letters*, *36*, L11606. https://doi.org/10.1029/2009GL038304

Xue, Z., He, R., Fennel, K., Cai, W.-J., Lohrenz, S., Huang, W.-J., … Zang, Z. (2016). Modeling pCO2 variability in the Gulf of Mexico. *Biogeosciences Discussions*, *13*, 4359–4377. https://doi.org/10.5194/bg-13-4359-2016